MODELLING SOIL EROSION AND SEDIMENT YIELD AT A CATCHMENT SCALE: THE CASE OF MASINGA CATCHMENT, KENYA

B. M. MUTUA[1,2]* A. KLIK[1] AND W. LOISKANDL[1]

[1]*Institute of Hydraulics and Rural Water Management, University of Natural Resources and Applied Life Sciences, Vienna, 18 Muthgasse, 1190, Vienna, Austria*
[2]*Department of Agricultural Engineering, Egerton University, Box 536, Njoro, Kenya*

ABSTRACT

Development of improved soil erosion and sediment yield prediction technology is required to provide catchment stakeholders with the tools they need to evaluate the impact of various management strategies on soil loss and sediment yield in order to plan for the optimal use of the land. In this paper, a newly developed approach is presented to predict the sources of sediment reaching the stream network within Masinga, a large-scale rural catchment in Kenya. The study applies the revised universal soil loss equation (RUSLE) and a developed hillslope sediment delivery distributed (HSDD) model embedded in a geographical information system (GIS). The HSDD model estimates the sediment delivery ratio (SDR) on a cell-by-cell basis using the concept of runoff travel time as a function of catchment characteristics. The model performance was verified by comparing predicted and measured plot runoff and sediment yield. The results show a fairly good relationship between predicted and measured sediment yield ($R^2 = 0.82$). The predicted results show that the developed modelling approach can be used as a major tool to estimate spatial soil erosion and sediment yield at a catchment scale. Copyright © 2006 John Wiley & Sons, Ltd.

KEY WORDS: soil erosion modelling; sediment yield; catchment management; RUSLE; GIS; Sediment Delivery Ratio; HSDD; Kenya

INTRODUCTION

Soil erosion is a natural geomorphic process that can be accelerated under improper land use and management practices. Problems caused by soil erosion and sediment yield include loss of soil productivity, water quality degradation, and less capacity to prevent natural disasters such as floods. Apart from reducing the water storage capacity, sediment delivered into water bodies may also be a source of contamination, adversely impacting the aquatic biota (Novotny and Olem, 1994).

As land degradation has become more evident with increasing changes in land use and management practices within Masinga catchment, the area of the present study, it has become necessary to spatially quantify soil erosion and sediment yield at the catchment scale. This is to assist in identifying and prioritizing areas that require immediate conservation measures. To improve water resources development, achieve sustainable land use and land productivity in Masinga, an integrated catchment management approach is needed. Development of improved soil erosion prediction technology is required to provide conservationists, farmers and other land users with the tools they need to evaluate the impact of various management strategies on soil loss and sediment yield, and plan for the optimal use of the land.

---

*Correspondence to: B. M. Mutua, Department of Agricultural Engineering, Egerton University, Box 536, Njoro, Kenya.
E-mail: bmmutua@yahoo.com

Objectives

The objectives of this paper are (a) to present a methodology that integrates the RUSLE and the HSDD model in a GIS environment to estimate the spatial distribution of soil erosion and sediment yield at a catchment scale, and (b) to demonstrate the use of this methodology by applying it to Masinga, a typical rural catchment in Kenya.

MATERIALS AND METHODS

Study Area

The Masinga catchment area (Figure 1) is some $6262\,km^2$, lying to the east of the Aberdare Mountains and south of Mount Kenya. It is located between latitudes $0°7'$ and $1°15'S$, and longitudes $36°33'$ and $37°46'E$. The elevation ranges on from 900 to 4000 m (a.m.s.l.). The catchment falls within five agro-climatic zones of Kenya, ranging from semiarid in the east to humid on the western side. The mean annual rainfall varies from about 600 to 2000 mm with mean annual temperatures ranging from 21 to 31°C. The catchment has an estimated population of 2 million people (Opiyo, 1999). Most people engage in agricultural and grazing activities, which take about 86 per cent of the total catchment area (Mutua, 2005).

Predicting Soil Erosion

As is common to many tropical countries, Kenya lacks sufficient financial resources to research and monitor outcomes of environmental degradation at a catchment scale. Most erosion assessment approaches in Kenya have in the past used runoff plot level observations to extrapolate catchment or landscape unit erosion rates (Grunblatt *et al.*, 1991). Although the runoff plots provide good experimental insight into the relationships between soil loss under different cover, soils and slopes, their results cannot be extrapolated for the entire catchment.

Modelling soil erosion provides an alternative and a sophisticated tool for selecting appropriate soil conservation practices especially at large catchment or regional scales. Recent advances in the use of geographical information system (GIS), remote sensing (RS) and the digital elevation model (DEM) have promoted the development and application of spatially distributed models of soil erosion and sediment delivery at the catchment scale (Nearing *et al.*, 1989; Ferro and Minacapilli, 1995; Perrone and Madramootoo, 1999). Use of a distributed approach permits both the spatial heterogeneity of catchment land use, soil properties and topography and the spatial variability and interaction of erosion and sediment delivery processes to be represented. This helps to provide spatially distributed predictions of soil erosion and sediment redistribution for complex three-dimensional terrains (Kothyari and Jain, 1997; De Roo, 1998; Parson and Stromberg, 1998).

One important limitation of applying the available process-based models has, however, been the lack of data for model parameterisation, validation and, more particularly, for validating the spatial pattern of sediment redistribution within a large rural catchment. Physically distributed models are mostly applied to small catchments, for example: WEPP (Laflen *et al.*, 1991); LISEM (De Roo *et al.*, 1996); EUROSEM (Morgan *et al.*, 1998), which are represented by a good data basis. This kind of data is lacking in most large rural catchments such as Masinga.

Modelling Approach

The present study area lacks extensive data, a requirement for the available physically distributed models. A modelling approach that captures the behaviour of the catchment utilising the available data was therefore chosen and applied to estimate the soil erosion rates. A simplified but physically distributed component was developed and incorporated with the revised universal soil loss equation (RUSLE) to predict the sediment yield in a spatial domain. The RUSLE model was chosen in this study because its data requirements are not too complex or unattainable, it is relatively easy to parameterise, and it is compatible with GIS.

The RUSLE is a lumped parameter model. It lumps spatial and temporal factors into an average number across a varying landscape (Renard *et al.*, 1997). The inputs to RUSLE model are geographically dependent and can be created as separate layers, which can be processed within a raster GIS (Cowen, 1993). Use of GIS platform has
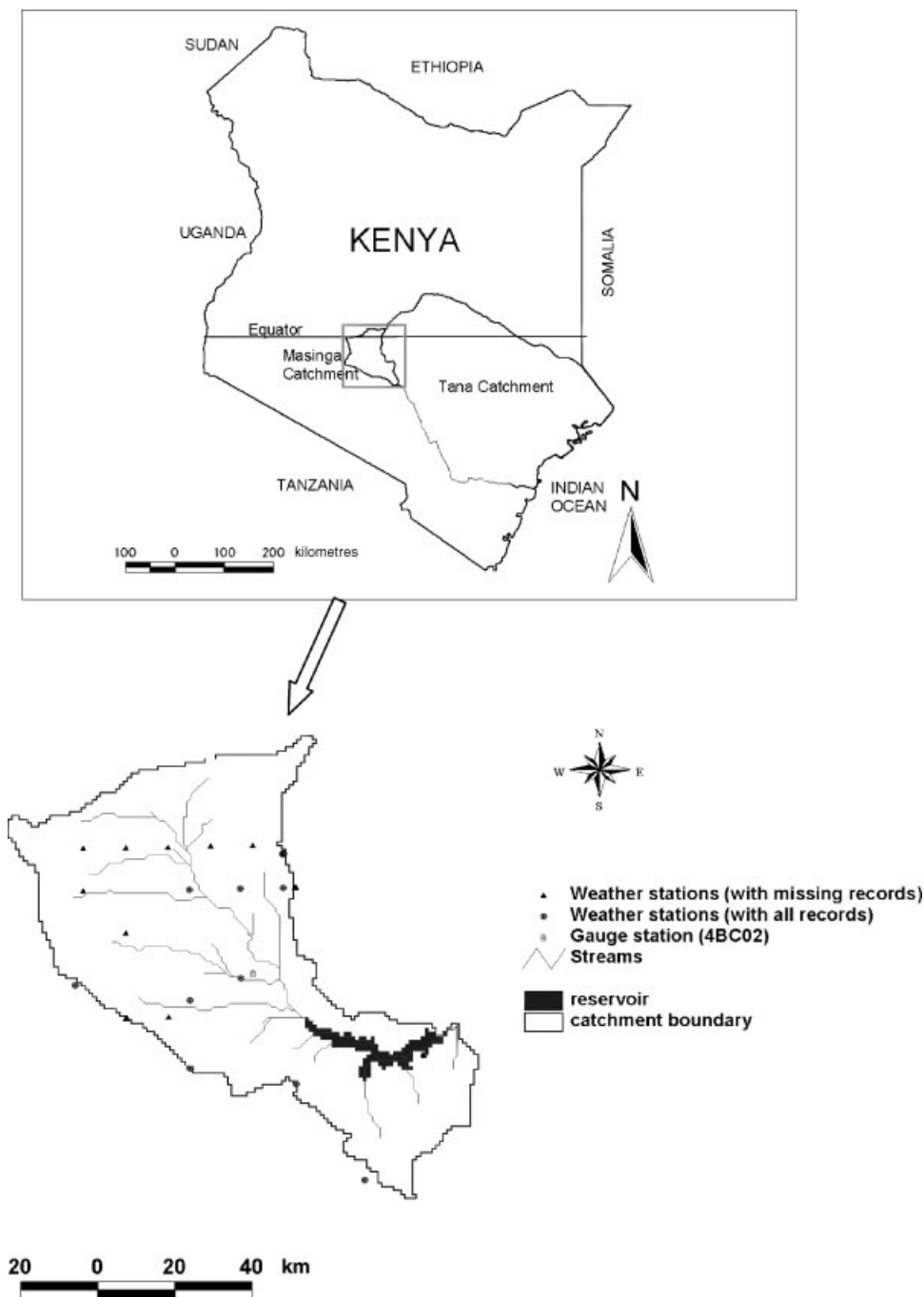
Figure 1. Location of study area on the Kenyan map.

therefore liberated the RUSLE model from its spatial and technological limitations (Maidment, 1993; Millward and Mersey, 1999) by allowing cell-by-cell spatial analysis.

In order to model the catchment behaviour, simplifications or generalisation must be made at some level to reduce real-world situations to model capabilities. A raster GIS adequately represents the changes within these

environmental landscape variables as well as defines a scale at which these changes occur. It allows analysis at each selected grid cell.

In this study, the mean annual gross soil erosion was calculated at a cell level in a raster GIS using six factors, which are composite factors of many others. These six factors are expressed in the RUSLE model structure:

$$A_i = LS_i \; R_i \; K_i \; C_i \; P_i \tag{1}$$

where subscript i is the ith cell; A (t ha^{-1} year^{-1}) is the estimated mean annual soil loss; LS is the combination of the slope steepness and slope length factors; R (KJ mm m^{-2} h^{-1} year^{-1}) is the erosivity factor; K (t ha^{-1} KJ^{-1} mm^{-1} m^2 h) is the soil erodibility factor; C is the cover and management factor and P is the support practice factor.

Five primary data themes were used to generate the RUSLE factors. These were the digital elevation model (DEM), the climatic data (precipitation), soil data, land use/cover and conservation support practices. The DEM was required to derive the slope length (L) and the slope steepness (S) factors. The rainfall erosivity (R) factor was derived from climatic data; the soil erodibility (K) factor from the soil type; the crop management (C) factor from land use/cover and the conservation practice (P) factor was estimated from available data provided by the Kenyan Ministry of Agriculture. All these model factors were generated in digital form and imported together with their associate attribute tables into Arc View$^{\circledR}$ GIS platform.

One major improvement made in the RUSLE model in this study was the application of upslope-area contributing method in determining the slope length and steepness factors. This modification made the model to act on a semi-distributed form. In the RUSLE modification, a simpler continuous form of equation for computing the LS-factor for each grid cell based on the catchment DEM was applied. The equation is given as:

$$LS_i = (m+1) \left[\frac{A_{i,j}}{a_o} \right]^m \left[\frac{\sin \theta_{i,j}}{b_o} \right]^n \tag{2}$$

where $A_{i,j}$ (m^2 m^{-1}) is the unit contributing area of a grid cell (i,j), $\theta_{i,j}$ is the slope angle, $a_o = 22 \cdot 1$ (m) and $b_o = 9$ per cent (for standard USLE plot), $m = 0 \cdot 6$ and $n = 1 \cdot 3$ are parameters (after Mitasova *et al.*, 1996). The flow direction and accumulation grid layers established from the DEM, and the cell size of 90 m based on DEM resolution were used to estimate the unit contributing area.

The use of time-series of remote sensing imagery and daily rainfall to incorporate the effects of seasonally varying rainfall intensity allowed for the estimation of spatial seasonal erosivities in Masinga catchment. The seasonal erosivities were estimated using a daily rainfall model based on erosive daily precipitation (Mutua, 2005). The daily rainfall model is given as:

$$\mathrm{EI}_{30}(j) = \alpha[1 + \eta \cos(2\pi f j - \omega)] \sum_{d=1}^{N} R_{\mathrm{d}}^{\beta}, \quad \text{for } R_{\mathrm{d}} \geq R_o \tag{3}$$

where $\mathrm{EI}_{30}(j)$ (KJ mm m^{-2} h^{-1}) is the jth monthly erosivity, R_{d} (mm) is the daily rainfall amount, R_o (set to $12 \cdot 7$ mm) is the threshold rainfall amount to generate runoff. The storm events, which have total rainfall depth equal or greater than $12 \cdot 7$ mm are considered to be potentially harmful in terms of soil erosion and sediment transport especially in tropical climates. N is the number of days with rainfall amount $\geq R_o$. α, β, η and ω are model parameters. The first part of Equation (3) is a sinusoidal function with a wavelength of 12 months and a fundamental frequency $f = 1/12$. This part of the equation is used to describe the seasonal variation of rainfall erosivity.

The model parameter α for the case of R_o 12·7 mm, was computed for each rainfall station within the catchment using the expression:

$$\alpha = 0 \cdot 395 \left[1 + 0 \cdot 098 \exp\left(3 \cdot 26 \frac{\Psi}{M_R} \right) \right] \tag{4}$$

where $\beta = 1 \cdot 49$, $\eta = 0 \cdot 29$ (adapted from Yu {1998} for tropical countries), M_R (mm) is the mean annual rainfall and Ψ is the mean for the long rains (March to May for Masinga area). In this study, the parameter ω in Equation (3) was set at $2\pi/3$ implying that for a given amount of daily rainfall, the corresponding rainfall erosivity is highest in April, for most parts of Masinga catchment. For each year, the total monthly EI_{30} values for each station were computed and an average value was determined as R-factor. A spatial rainfall erosivity map was created by interpolation of the point theme R-factors using the inverse distance weighting (IDW) interpolation method, a procedure supported by Arc View® GIS.

The generated RUSLE data themes and their associated attribute tables were integrated in the ArcView RGIS to predict the average annual soil loss for the catchment. The analytical and manipulation tools within the GIS allowed for the quantification of the parameters from available data sets. The generated soil erosion layer was overlaid with the spatial sediment delivery ratio layer (described in the following section) to estimate the mean annual sediment yield.

ESTIMATING SPATIAL SEDIMENT DELIVERY RATIO (SDR)

Sediment yield is not usually available as a direct measurement. It is usually estimated using a sediment delivery ratio (SDR) concept. SDR is a measure of sediment transport efficiency, which accounts for the amount of sediment that is actually transported from the eroding sources to a measurement point or catchment outlet, compared to the total amount of soil that is detached over the same area above that point.

There is no precise procedure for estimating SDR, although the USDA-SCS (USDA, 1972) published a handbook in which the SDR is related to drainage area. One of the most widely used methods to estimate SDR for large scale catchments, is the empirical SDR-area power function:

$$\text{SDR} = \alpha A^\beta \tag{5}$$

where A (km²) is the catchment area, and the constant α, and a scaling exponent β are empirical parameters (Maner, 1958; Roehl, 1962). Field data from studies carried out in different catchments of the world show that the relationship between SDR and drainage area changes considerably for each catchment.

Most of the empirical models for estimating SDR were developed after many years of plot runoff measurements in small-scale catchments. Application of such empirical SDR models is limited in large rural catchments such as Masinga. Masinga catchment has very few runoff plots and in addition, there is very little sediment yield data available to calibrate the parameters of the SDR-area based models.

Faced with such a limitation, the solution lies in the development of a spatially distributed sediment delivery model with modest input parameter requirement. In this study therefore, a physically distributed sediment delivery model, the hillslope sediment delivery distributed (HSDD) was developed. The HSDD model, which is a simplified sediment transport model, applies the concept of runoff travel time to estimate a spatial SDR grid layer. Such a concept has been applied in other studies (Ferro and Porto, 2000).

The HSDD model is a GIS-based technique for deriving unique spatially sediment delivery ratios through grid-based layers. The model requires the discretisation of the catchment into hydrological units (sub-catchments with same hydrological properties). To apply HSDD model, Masinga catchment was therefore delineated and discretised into morphological units (i.e. areas of defined aspect, length, steepness) using the spatial and hydrological tools in Arc View® software. For model computation, the discretised polygons were rasterised
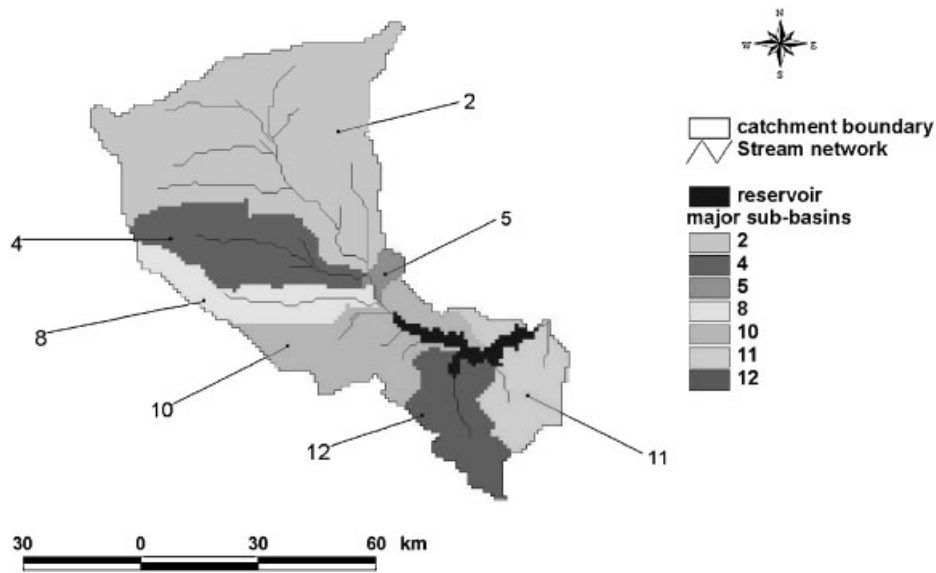
Figure 2. Discretised sub-catchments as grid layers.

and then aggregated into seven major sub-catchments (Figure 2) based on the pour points (outlets) of the delineated stream network.

A relationship between the SDR and the sediment travel time expressed as a function of the overland and channel flow, and sub-catchment response coefficient was developed. This relationship is given as:

$$\text{SDR} = \exp(-\beta T) \tag{6}$$

where β is the sub-catchment response coefficient, T (hr) is the sum of the overland travel time t_o and the shallow concentrated flow travel time t_c of the sediment. It was assumed that the sediment that reaches the stream network takes the same travel time as the runoff.

This study focused on creating an infiltration-excess runoff model entirely within Arc View® GIS. One of the most important input grid layers to HSDD model is the sub-catchment response coefficient, β. This was generated using a physically distributed hydrologic model, the stream flow model (SFM). The SFM was developed using the 'C' programming language. The user interface for the SFM was realised by the avenue script and loaded as an extension to the standard Arc View® graphical user interface. The advent of object-oriented GIS programming languages has broken the barrier to capturing time variation of spatial processes that was so far a limitation in earlier GIS applications in hydrology. GIS has improved the efficiency of hydrologic modelling, most notably in the representation of terrain, which depicts water flow and transport patterns in a particular cell (Maidment, 1993).

HSDD Model Input

The basic input data layers for HSDD model are a DEM, precipitation, evaporation, land use/cover and soil data. In addition, the model requires data describing the average water holding capacity of the soils (cm), average hydrologically active soil depth (cm), textural description of the soil, average saturated soil hydraulic conductivity (cm hr^{-1}) and average curve number. These were obtained from Africa database developed by USGS, FAO soil database (FAO-UNESCO, 1998) and from other relevant departments such as Soil Survey of Kenya (SSK).

In this study, the spatial curve numbers were determined by first merging the soil groups and land use/cover files which formed a common field. The Arc View® 'field calculator' was then used to estimate the curve numbers

Table I. Relationship between land cover, hydrologic soil group combinations and runoff curve numbers

Land cover description	Soil group A	Soil group B	Soil group C	Soil group D
Urban and built-up land	73	82	88	90
Dryland cropland and pasture	71	80	86	86
Irrigated cropland and pasture	64	74	81	84
Cropland/grassland mosaic	63	73	82	87
Cropland/woodland mosaic	51	68	78	82
Grassland	60	76	81	89
Shrubland	48	62	73	78
Savanna	44	65	77	82
Deciduous broadleaf forest	55	66	74	79
Evergreen broadleaf forest	55	66	74	79
Water bodies	100	100	100	100
Herbaceous wetland	100	100	100	100
Wooded wetland	100	100	100	100
Barren or sparsely vegetated	75	80	85	90

based on a relationship between the SCS curve numbers, the four hydrologic soils groups, and land use/cover types (Table I).

Arc View® SFM extension provides a common interface for model pre-processing of catchment and hydrometeorological data, model set up and execution as well as post-processing of model output. One of the main hydrometeorological data sets used in this study was the daily rainfall and evaporation data. These geo-referenced data were pre-processed and then used as an input layer into the Arc View® SFM extension to estimate the catchment water balance.

The Arc View® SFM couples a runoff generation sub-component based on the soil conservation service (SCS) approach and a DEM-based travel time routing method. The SFM has an upland headwater basin-routing module and a major river-channel routing module. The model first determines the excess amount of precipitation. That is, the amount of precipitation falling on the catchment that cannot be infiltrated into the soil layer. The model determines how much water enters the stream network from each sub-catchment. Within the sub-catchments, the surface runoff is simulated using a source-to-sink method, while subsurface contributions to stream flow are simulated with two conceptual linear reservoirs (Figure 3). In the major river channels, the runoff is routed using a non-linear Muskingum-Cunge scheme (Cunge, 1969; Dooge *et al.*, 1982; Wilson, 1990).

The time for runoff water to travel from one point to another over the catchment was determined using the flow distance and velocity along the flow paths. The equation used for the overland flow given as:

$$t_o = \sum_{i=1}^{N_p} \frac{l_i}{v_i} \qquad (7)$$

where t_o (hr) is the travel time through the grid cells, l_i (m) is the length of segment i in the flow path, v_i (m s^{-1}) is the flow velocity in cell i and N_p is the number of cells traversed by runoff from cell i to the nearest channel. For a cell i, the cumulative travel time was estimated by summing the travel time along its flow path (based on the flow direction). The flow length was determined by using the flow direction and flow accumulation grid layers.

The surface runoff (excess rainfall) was estimated based on the SCS curve number method:

$$Q_i = \frac{(P_i - 0 \cdot 2S_i)^2}{P_i + 0 \cdot 8S_i}, \quad \text{for } P > 0 \cdot 2S \qquad (8)$$
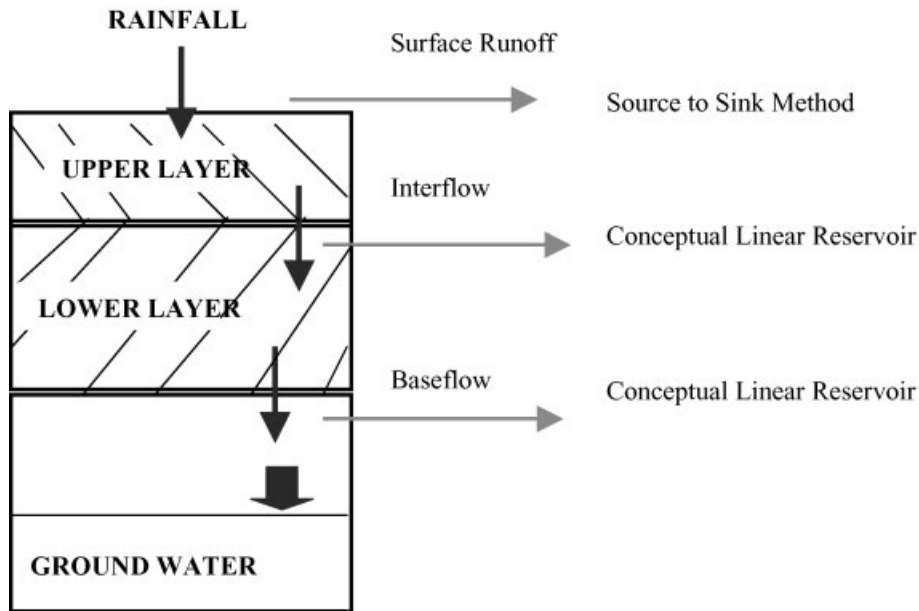
Figure 3. Simulation of the contribution of surface and sub-surface flow to a stream network.

where subscript i is the ith cell, Q (mm) is the daily runoff, P (mm) is the daily rainfall, CN is the grid curve number. S (mm) is the retention parameter estimated using the relation:

$$S_i = 254\left(\frac{100}{\mathrm{CN}_i} - 1\right) \tag{9}$$

The overland flow velocity was estimated using the kinematic wave equation. A modified velocity equation was used based on land use type and land slope. Each land use/cover type was assigned a velocity coefficient. These coefficients α_i (Table II) were adapted from values given by McCuen (1998). The velocity was estimated using the relation:

$$v_i = \alpha_i s_i^{1/2} q_i \tag{10}$$

where v_i is runoff velocity (m s^{-1}), s_i (m/m) is slope of cell i and q_i (m s^{-1}) is specific runoff rate (i.e. runoff rate per unit cell area).

Table II. Relationship between land cover description and velocity coefficient α

Land cover description	Velocity coefficient
Urban and built-up land	6·3398
Dryland cropland and pasture	0·4572
Irrigated cropland and pasture	2·7737
Cropland/grassland mosaic	0·3962
Cropland/woodland mosaic	0·3962
Grassland	0·6401
Shrubland	0·4572
Savanna	0·4267
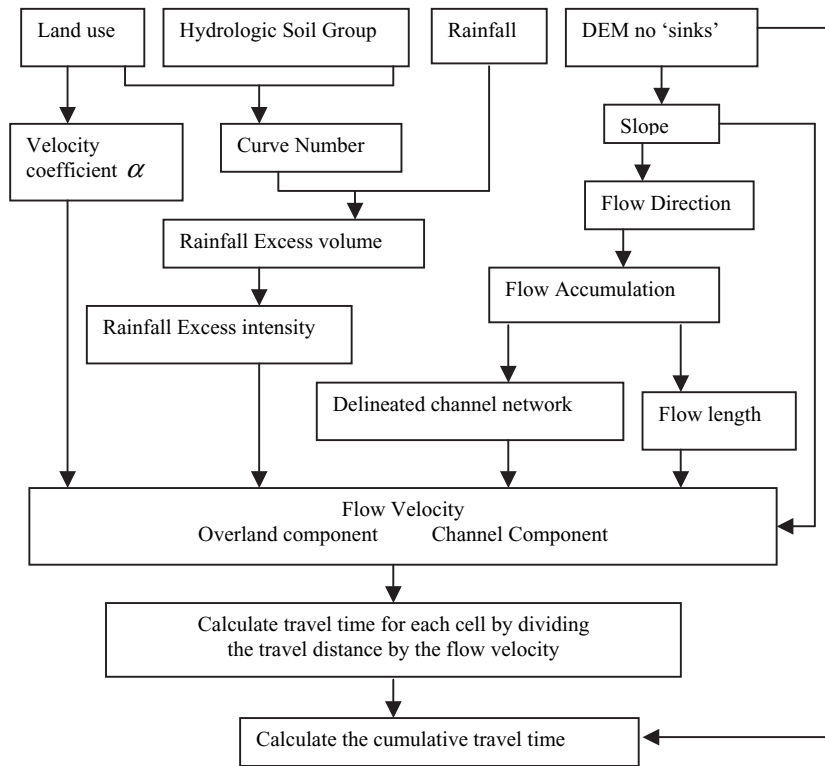
Figure 4. Flow chart for the calculation of the travel time for the sediment particles.

The conceptual procedure for estimating the cumulative travel time of the sediment is given in Figure 4. Table III presents a summary of the main average physical properties of the discretised sub-catchments.

RESULTS AND DISCUSSION

Spatial Mean Annual Soil Erosion Results

The spatial grid themes (R, LS, K, C and P) were multiplied together using the ArcView's map calculator to generate the spatial soil erosion map (Figure 5). The quantitative output of the predicted soil erosion rates for the

Table III. Main average attributes of the discretised sub-catchments for Masinga

Basin ID	Soil WHC (mm)	Soil depth (cm)	Area (km^2)	Hlength (m)	Hslope (m)	UpArea (km^2)	Elevation (m)	SCS number CN	Max cover (%)	Manning coefficient
2	117·178	94·4	2758	21 776·3	1·6912	2757	2143·9	76·4	0	0·065
4	126·942	101·0	821	23 002·3	1·9787	820	1897·4	73·3	0	0·045
5	63·8816	102·9	76	5312·6	0·6324	3654	1198	79·8	0	0·025
8	108·168	97·9	506	34 384	1·865	505	1802·5	73·1	0	0·035
10	77·8595	121·9	918	16 939·1	0·901	5078	1309·9	76·9	0·00106	0·035
11	112·868	195·4	597	13 419·6	0·874	6261	1121	73·9	0·00147	0·075
12	88·6997	150·2	586	18 397·8	0·9661	585	1213·9	75·4	0·00106	0·055

WHC, water holding capacity; Hlength, hillslope length; Hslope, hillslope (m/100 m); UpArea, upslope contributing area; SCS, soil conservation service curve number; max cover, maximum portion of land cover that is impervious.
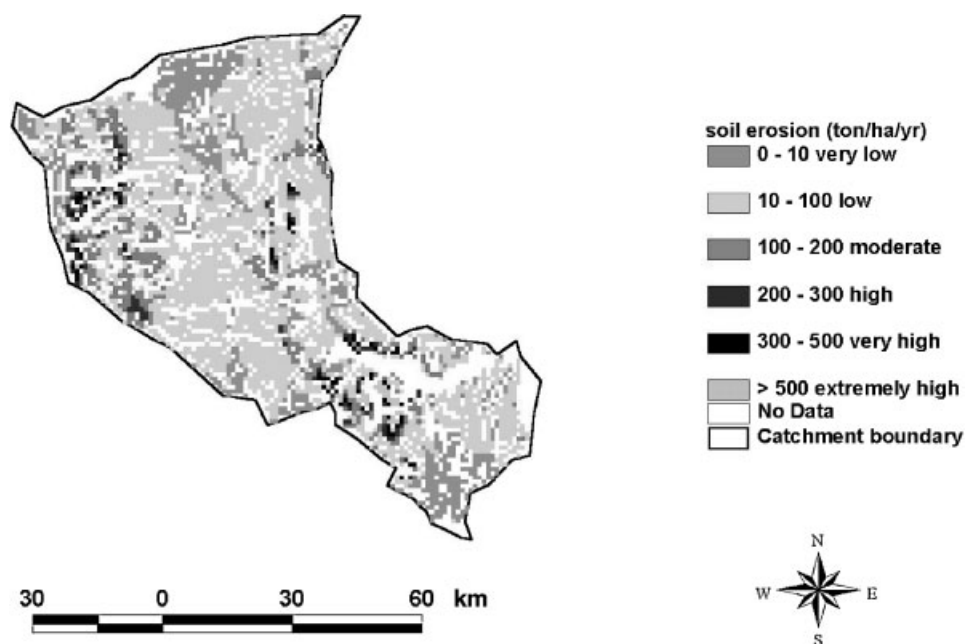
Figure 5. Predicted spatial mean annual soil erosion within Masinga catchment.

Masinga catchment resulting from the land use/cover and management practices for 2004 were computed and grouped into six ordinal classes (Table IV).

The critical areas that require urgent soil and water conservation management are easily identified from the spatial erosion map (Figure 5). The areas experiencing moderate to very high soil erosion rates are in the northwest, western, south eastern and a bit of the eastern zones of the catchment. The estimated annual soil loss tolerance (*T*) for most Kenyan rural catchments ranges from 2·2 to 10 t ha^{-1} year^{-1} (Angima *et al.*, 2003). Based on the standard classification and gradation of soil erosion in Kenya, the results in Table IV show that only 9·3 per cent of the total catchment area is experiencing soil erosion within the tolerable rates.

From the spatial soil erosion map, (Figure 5), it can be inferred that the present land utilisation with lack of soil conservation measures, a rather low standard of husbandry on arable land, gross overstocking and lack of management on range lands is resulting in high soil erosion.

Spatial Sediment Delivery (SDR) Results

When the model was run, a spatial SDR map for Masinga catchment (Figure 6) was generated. Figure 6 shows that far away cells contribute less sediment delivery to stream network. Travel time is calculated from velocity. Hence two locations that are equidistant from the outlet may not have the same travel time, that means in general travel

Table IV. Results of soil erosion for 2004 land use and management practices

Soil class	Soil loss range (t ha^{-1} year^{-1})	Description of soil loss class	Area (km^2)	Catchment area (%)	Mean
1	0–10	Very low	582	9·3	5·11
2	10–100	Low	2628	42·0	40·49
3	100–200	Moderate	522	8·3	137·78
4	200–300	High	116	1·9	240·03
5	300–500	Very high	101	1·6	379·66
6	> 500	Extremely high	57	0·9	779·13
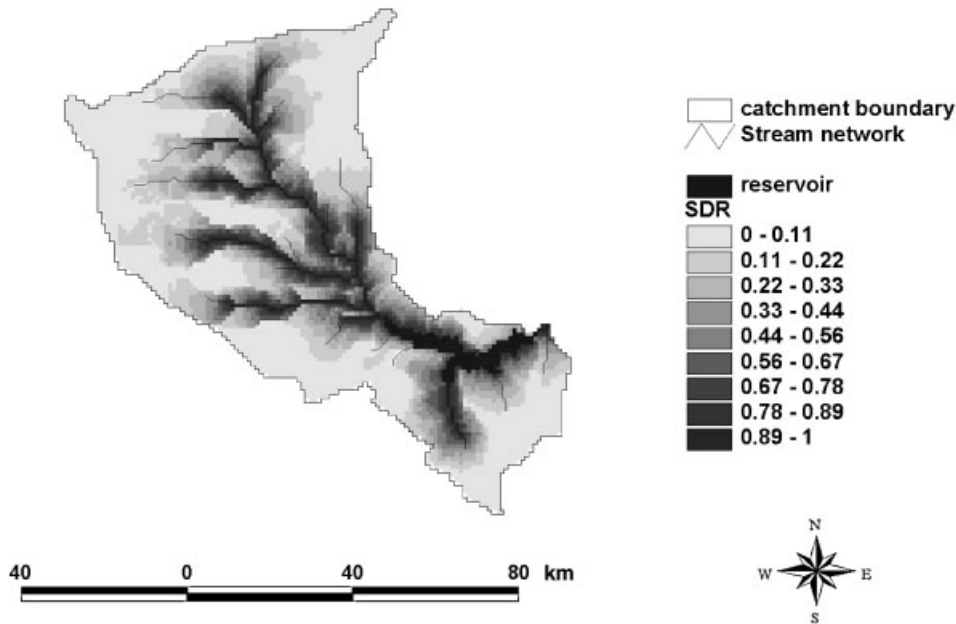
Figure 6. Predicted spatial sediment delivery ratio in Masinga catchment.

time does not follow concentric zones. Flow velocity in reality is controlled by conditions such as the surface vegetation type and roughness and elevation changes over the drainage area. Thus longer travel time will tend to occur in areas with rougher surfaces (vegetated areas) compared with bare and open land surfaces.

The simulated SDR varies from 0·0 to 1·0 within the sub-catchments with an overall value averaged for all the grid cells for the catchment being 0·29. The sediment delivery ratio values imply the integrated capability of a basin for storing and transporting the eroded soil.

Estimated Spatial Sediment Yield

The SDR grid layer was overlaid with the mean annual soil erosion grid layer and the output was a grid layer (Figure 7) depicting sediment yield reaching the stream network within Masinga catchment. The sources of sediment yield are clearly identified in a spatial domain. These sources of high sediment coincide well with areas under intensive cultivation and steep slopes. Most of the sediment reaching the main channel is produced from the cropland. The western part of the catchment has the highest rainfall and steep slopes and because of the intensive cultivation, a lot of soil is lost through erosion. Some parts of the eastern area of the catchment are also contributing high yields of sediment. There are some areas in the southeast of the catchment especially near Masinga reservoir where high-sediment yield is predicted. Although some of these southeastern areas have gentle slopes and low mean annual rainfall, the poor land husbandry and the intensive overgrazing can be attributed to the high-sediment yield.

The predicted results show a great variation in sediment yield within each sub-catchment (Table V). Such high variations are a result of the diverse land use practices, wide range of land slopes and distance to channels within the individual sub-catchments. Those sub-catchments in which forest and grass are the principal land cover produce low-soil erosion and sediment yield, although some of these sub-catchments have relatively high-sediment delivery ratios.

The predicted average sediment yields at each sub-catchment outlet show that the sediment yield does not depend entirely on the sub-catchment area (see Table V). For instance, sub-catchment number 4 whose area is 821 km^2 has a mean annual sediment yield of about 84·7 t ha^{-1} year^{-1} compared to 77·9 t ha^{-1} year^{-1} for sub-catchment number 2 with an area of 2758 km^2. This shows that the general method of estimating SDR based on the
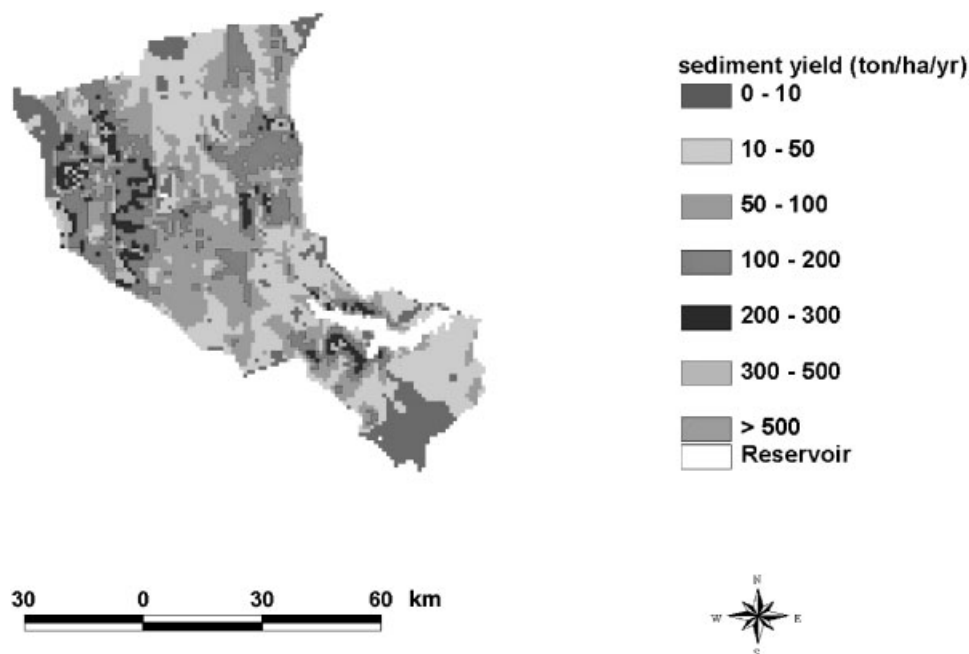
Figure 7. Predicted spatial mean annual sediment yield within Masinga catchment.

drainage catchment area is not reliable especially for a large catchment with varied characteristics such as Masinga.

   Results of Table V show that the average sediment yield at the sub-catchments' outlets can only give an overall sediment yield reaching the outlet which cannot be used to explain the spatial variation of sediment over the sub-catchment. For example, in sub-catchment 10, the mean annual sediment yield varies between 2·3 and 331·6 t ha^{-1} year^{-1} with an average of 30·6 t ha^{-1} year^{-1} at its outlet compared to sub-catchment 8 whose mean annual sediment yield varies between 16·1 and 158·7 t ha^{-1} year^{-1} with an average of 50·3 t ha^{-1} yr^{-1} at its outlet. Although there is a wide variation in sediment yield in sub-catchment 10, not all sediment reach its outlet. This means that most of the sediment in hillslope with low slopes is deposited before reaching the main stream at the outlet.

Table V. Variation of sediment yield within the sub-catchments in Masinga

		Mean annual sediment yield (t ha^{-1} year^{-1})	
Sub-catchment No.	Area (km^2)	Sediment variation within sub-catchment	Mean sediment yield at sub-catchment outlet
2	2758	8·9–242·9	77·9
4	821	10·3–501·7	84·7
5	76	2·9–51·8	9·7
8	506	16·1–158·7	50·3
10	918	2·3–331·6	30·6
11	597	1·0–106·1	17·9
12	586	1·8–84·8	14·8
Total area = 6262			* Average = 57·2

*Overall average annual sediment yield (t ha^{-1} year^{-1}) based on weighted area.
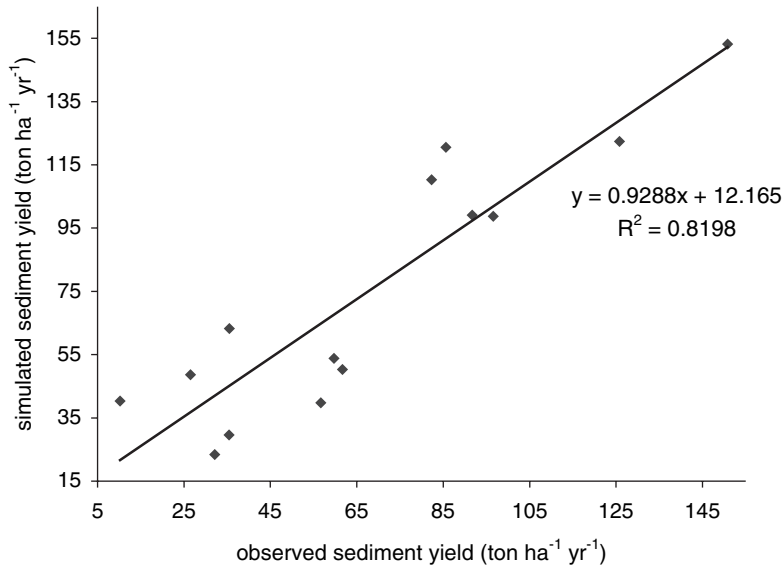
Figure 8. Comparison between measured and predicted mean annual sediment yield.

Model Verification

The mean annual soil loss generated by the RUSLE-GIS model is subject to error due to inaccuracies inherent in each data layer, and the limitations of the methods used to derive values for each component. This calls for the verification of the model to determine its prediction performance. A quantitative and a visual field survey was conducted within the study area between November 2004 and January 2005. For each sub-catchment, a number of runoff plots were identified and used. A visual observation was also done to compare the predicted and the observed erosion within each sub-catchment. Visual observation showed that the model predicted the mean annual soil erosion fairly well. Measured sediment yields from the runoff plots within the sub-catchments were compared with predicted results. Figure 8 shows the relationship between predicted and measured mean annual sediment yields from some of the runoff plots within the catchment.

The results show a fairly good relationship (coefficient of regression $R^2 = 0.82$) between the predicted and observed sediment yield. The results in this study are based on the model before it was calibrated and it is envisaged that better model performance could be attained after its calibration.

CONCLUSIONS

This study presents a simplified approach of predicting soil erosion and sediment yield for a large rural catchment. The developed approach allows for the identification of primary sediment source areas and the sediment yield reaching the stream network. As opposed to the traditional SDR-drainage area method for an entire catchment, the developed spatially distributed SDR model based on the concept of the runoff travel time on a cell-by-cell basis, helps to identify and clarify those critical areas with high potential for sediment transport. The results show that the RUSLE and the developed HSDD models integrated in a GIS environment can be used to facilitate fast and efficient assessment of soil erosion and sediment yield, and thus can serve as a useful tool in natural resources management and planning for large-scale catchments. There is however, a need for further field research to improve the model performance through calibration and validation.

REFERENCES

Angima SD, Scott DE, O'Neill MK, Ong CK, Weesies GK. 2003. Soil erosion using RUSLE for central Kenyan highlands conditions. *Agricultural Ecosystems and Environment* **97**: 295–308.

Cowen J. 1993. *A proposed method for calculating the LS factor for use with the USLE in a GRID-BASED environment*: 1993 Environmental Systems Research Institute User Conference Proceedings, 65–74.

Cunge JA. 1969. On the subject of a flood propagation computation method (Muskingum Method). *Journal of Hydraulic Resources* **7**: 205–230.

De Roo APJ, Wesseling CG, Ritsema CJ. 1996. LISEM: a single event physically-based hydrologic and soil erosion model for drainage basins. I: theory, input and output. *Hydrological Processes* **10**: 1107–1117.

De Roo APJ. 1998. Modelling runoff and sediment transport in catchments using GIS. *Hydrological Processes* **12**: 905–922.

Dooge JCI, Strupczewski WG, Napiorkowski JJ. 1982. Hydrodynamic derivation of storage parameters for Muskingum model. *Journal of Hydrology* **54**: 371–387.

FAO-UNESCO. 1998. Soil Map of the World, Revised Legend, *FAO World Soil Resources Report No. 60.* Food and Agricultural Organisation of the United Nations, UNESCO, Rome.

Ferro V, Minacapilli M. 1995. Sediment delivery processes at basin scale. *Hydrological Sciences Journal* **40**: 703–716.

Ferro V, Porto P. 2000. Sediment delivery distributed (SEDD) model. *Journal of Hydraulic Engineering* **5**: 633–647.

Grunblatt J, Ottichilo WK, Sinange RK. 1991. A GIS approach to desertification assessment and mapping. *Journal of Arid Environments* **23**: 81–102.

Kothyari UC, Jain SK. 1997. Sediment yield estimation using GIS. *Hydrologic Sciences Journal* **42**: 833–844.

Laflen JM, Lane LJ, Foster GR. 1991. WEPP: a new generation of erosion prediction technology. *Journal of Soil and Water Conservation* **46**: 34–38.

Maidment DR. 1993. GIS and Hydrologic Modeling. In *Environmental Modeling with GIS*, Goodchild MF, Parks BO, Steyaert LT (eds). Oxford University Press: Oxford; 147–167.

Maner SB. 1958. Factors affecting sediment delivery rates in the Red Hills physiographic area. *Transaction of American Geophysics* **39**: 669–675.

McCuen RH. 1998. *Hydrologic Analysis and Design*. Prentice-Hall, Inc.: Upper Saddle River, NJ.

Millward AA, Mersey JE. 1999. Adapting the RUSLE to model soil erosion potential in a mountainous tropical watershed. *Catena* **38**: 109–129.

Mitasova H, Hofierka J, Zlocha M, Iverson LR. 1996. Modelling topographic potential for erosion and deposition using GIS. *International Journal of Geographical Information Science* **10**: 629–641.

Morgan RPC, Quinton JN, Smith RE, Govers G, Poesen JWA, Auerswald K, Chisci G, Torri D, Styczen ME. 1998. The European soil erosion model (EUROSEM): a dynamic approach for predicting sediment transport from fields and small catchments. *Earth Surface Processes and Landforms* **23**: 527–544.

Mutua BM. 2005. *Modelling Soil Erosion and Sediment Delivery to Reservoirs at a Large Scale domain, a Strategy for Catchment Management: The case of Masinga Catchment, Kenya*. Ph.D Thesis, University of Natural Resources and Applied Life Sciences (BOKU), Vienna.

Nearing MA, Foster GR, Lane LJ, Finkner SC. 1989. A process based soil erosion model for USDA-water erosion prediction project technology. *Transactions of the American Society of Agricultural Engineers* **32**: 1587–1593.

Novotny V, Olem H. 1994. *Water Quality: Prevention, Identification, and Management of Diffuse Pollution*. Van Nostrand Reinhold: New York, NY.

Opiyo CO. 1999. Challenges of Demographic Data Collection and Utilisation: the Case of the 1999 Kenya Population and Housing Census. *Population Association of Kenya Occasional Paper Series*, volume 1.

Parsons AJ, Stromberg SGL. 1998. Experimental analysis of size and distance of travel of unconstrained particles in interrill flow. *Water Resources Research* **34**: 2377–2381.

Perrone J, Madramootoo CA. 1999. Sediment yield prediction using AGNPS. *Journal of Soil and Water Conservation* **54**: 415–419.

Renard K, Foster G, Weesies G, McCool D, Yoder D. 1997. *Predicting soil erosion by water: a guide to conservation planning with the Revised Universal Soil Loss Equation (RUSLE)*. USDA Agriculture Handbook No.703. United States Government Printing Office, Washington, DC. 384.

Roehl JE. 1962. Sediment source areas, and delivery ratios influencing morphological factors. *International Association of Hydrological Sciences* **59**: 202–213.

USDA 1972. *Sediment Sources, Yields, and Delivery Ratios*. National Engineering Handbook, Section 3 Sedimentation. United state Department of Agriculture: Washington, DC.

Wilson EM. 1990. *Engineering Hydrology*. Macmillan: Indianapolis, IN, 110, 196, 301.

Yu B. 1998. Rainfall erosivity and its estimation for Australia's tropics. *Australian Journal of Soil Research* **36**: 143–165.